The High Aromatic and Stable Clusters Li5B, Li6B+/− and Li7B: A Case of the Phenomenological Shell Model

ARTICLE *in* CHEMICAL PHYSICS LETTERS · MAY 2010

Impact Factor: 1.9

2 AUTHORS:

Truong Tai

University of Leuven

67 PUBLICATIONS **524** CITATIONS

SEE PROFILE

Minh Tho Nguyen

University of Leuven

750 PUBLICATIONS **11,210** CITATIONS

SEE PROFILE

Chemical Physics Letters 489 (2010) 75–80

Contents lists available at ScienceDirect

Chemical Physics Letters

journal homepage: www.elsevier.com/locate/cplett

The high stability of boron-doped lithium clusters Li_5B, $Li_6B^{+/-}$ and Li_7B: A case of the phenomenological shell model

Truong Ba Tai [a], Minh Tho Nguyen [a,b,*]

[a] Department of Chemistry, LMCC-Mathematical Modeling and Computational Science Center, Katholieke Universiteit Leuven, B-3001 Leuven, Belgium
[b] Institute for Computational Science and Technology of HoChiMinh City, Thu Duc, HoChiMinh City, Viet Nam

ARTICLE INFO

Article history:
Received 11 January 2010
In final form 12 February 2010
Available online 17 February 2010

ABSTRACT

A quantum chemical investigation of the clusters Li_5B, Li_6B^+, Li_6B^- and Li_7B was performed using the DFT, MP2 and CCSD(T) methods. The high symmetry structures (C_{4v}, $^1A_1$), (O_h, $^1A_{1g}$) and (D_{5h}, $^1A_1'$) turnout to be the global minima for Li_5B, Li_6B^+ and Li_7B, respectively. These clusters are predicted to be highly stable species with large vertical ionization energies, and large HOMO–LUMO gaps. Chemical bonding of clusters was probed using an electron localizability indicator (ELI) which indicates a large aromatic character. The high stability of these clusters can be accounted for by the phenomenological shell model.

1. Introduction

Binary clusters composed of two types of elements have greatly been attractive, in part due to their wide range of interesting structural and electronic features [1–3]. It has been well-known that addition of impurities leads to fundamental changes in the geometry, electronic structure, energetic properties and thermodynamic stability of the doped clusters as compared to the bare host. The phenomenological shell model (PSM) which was proposed by Knight et al. [4], has proved to be an effective tool to interpret the variation with size of the properties of metal clusters [5–7]. In the framework of this model, the valence electrons are assumed to freely itinerant in a simple mean-field potential that is formed by the nuclei of atoms. Accordingly, the high stability of a metal cluster is as achieved if its electronic shells or sub-shells are closed, and the number of valence electrons corresponds to a shell closing such as 2 ($1S^2$), 8 ($1S^2$ $1P^6$), 20 ($1S^2$ $1P^6$ $1D^{10}$ $2S^2$), etc., that are called the *magic numbers*. However, this model was not successfully applied for some highly stable binary clusters of which number of valence electrons does not correspond to these magic numbers, such as K_8Zn [8], Na_6Pb [9]. A modified phenomenological (Wood-Saxon) potential was introduced as an extended model to explain the behaviour of these cases [10–12]. In this model, the dopant induces a perturbation and the ordering of the single particle energy levels is changed either to ($1S^2$ $1P^6$ $2S^2$ $1D^{10}$ $2P^6$) if the impurity is more electronegative than the host atoms, or to ($1S^2$ $1P^6$ $1D^{10}$ $2S^2$ $1F^{16}$ $2P^6$) if the central dopant is less electronegative than the host atoms.

Recently, lithium-based clusters have been investigated as a economic and simple model to approach the electronic structure of heavier metal clusters. A large number of the experimental and theoretical studies have been performed on pure lithium clusters [13,14] as well as on doped lithium clusters by many groups [15–17]. Theoretical investigations for boron-doped lithium clusters in both neutral and cationic states were performed by Nguyen et al. [18,19] and Li et al. [20,21]. Li et al. found that the neutral Li_5B was pointed out to have a high stability in the series of Li_nB clusters ($n = 1–7$), whereas the cation Li_6B^+ was found to have a high stability within the Li_nB^+ cationic cluster state. These authors [20,21] showed that the stability patterns of these systems can be interpreted using the spherical jellium model (SJM) [22] in which a high stability is expected for the systems possessing 2, 8, 20, 34, etc., valence electrons (called as the magic numbers) that correspond to the electron configuration $1s^2$ $1p^6$ $1d^{10}$ $2s^2$ $1f^{14}$. The SJM has accounted for the high stability of the clusters containing eight valence electrons such as Li_5B and Li_6B^+, but it was failed for larger systems. The HOMOs of Li_6B, Li_7B and Li_7B^+ are indeed found to be the s-orbitals that are not consistent with the energetic ordering of valence orbitals in the SJM. A fundamental difference between the PSM and SJM is that while the SJM treats the electron–electron interaction self-consistently in a positive background potential, the PSM is a one-electron approximation using confining potential. Thus in order to use the PSM, the Schrödinger equation for the one-electron-in-a-box problem needs to be solved using different box shapes.

In view of the fact that the PSM has been applied successfully for many binary clusters, a legitimate question is as to whether it can also be applied to rationalize the stability pattern of the Li_nB

* Corresponding author. Address: Department of Chemistry, LMCC-Mathematical Modeling and Computational Science Center, Katholieke Universiteit Leuven, B-3001 Leuven, Belgium. Fax: +32 16 32 79 92.
E-mail address: minh.nguyen@chem.kuleuven.ac.be (M.T. Nguyen).

0009-2614/$ - see front matter © 2010 Elsevier B.V. All rights reserved.
doi:10.1016/j.cplett.2010.02.036

clusters. In this work, we set out to tackle this question in carry out a theoretical investigation of electronic structure, chemical bonding and aromaticity of the species Li_5B and Li_7B and their isoelectronic systems Li_6B^+ and Li_6B^- using quantum chemical methods. Our calculated results reveal that the electronic structure of these stable clusters is consistent with the PSM. In addition, we also probe their aromatic character.

2. Computational methods

All electronic structure calculations were carried out using the Gaussian 03 [23] and Molpro 06 [24] suites of programs. Geometry optimizations and calculations of harmonic vibrational frequencies of the clusters considered were fully performed using density functional theory with the hybrid B3LYP functional [25] and the second-order Møller–Plesset perturbation theory [26] in conjunction with the correlation consistent aug-cc-pVTZ basis set. Total electronic energies of the lowest-lying isomers were subsequently calculated using the coupled-cluster theory CCSD(T) [27], which is a more reliable method for determining the relative energies between cluster isomers.

The analysis of the chemical bonding was performed using the electron localizability indicator (ELI) [28] and the canonical molecular orbitals (MOs). Similar to the electron localization function (ELF) approach, the ELI-D scheme [29] and its orbital decomposition are proved to be an effective tool to probe the chemical bonding in organic compounds as well as in transition metal compounds [30]. The ELI is defined as the integral of the electron density over micro-cell containing the same fraction of same-spin electron pairs. It can be considered to be a product of the pair volume function and the electron density, and is equal to a sum of orbital densities in the case of single determinant wave functions. Thus, the ELI-D can be decomposed into molecular orbital contributions that are called the partial electron localizability indicator (pELI). The ELI-D values were calculated by using Dgrid-4.2 program suite [31] and the ELI isosurfaces were plotted using the Gopenmol software [32].

3. Results and discussion

3.1. Global minima structures

A large variety of isomeric structures for the clusters Li_5B, Li_6B^+, Li_6B^- and Li_7B were initially optimized using the B3LYP/aug-cc-pVTZ level. Geometries of a few lowest-lying isomers were subsequently reoptimized using the MP2 and CCSD(T) methods, and their single point electronic energy calculated using the CCSD(T) method with the same aug-cc-pVTZ basis set. The optimized geometries, relative energies and number of imaginary frequencies for the lower-lying structures considered are depicted in Fig. 1, whereas their Cartesian coordinates are listed in Table S1 of the Supplementary material.

For Li_5B, our findings are in good agreement with previous studies [18,20] that the high symmetry structure (C_{4v}, $^1A_1$) is the most stable isomer. At the B3LYP/aug-cc-pVTZ level, the two structures having C_{2v} ($^2A_1$) and D_{3h} ($^2A_1'$) point groups turn out to be transition structures having the same energetic content, and are ~1.5 kcal/mol higher as compared to the global minimum.

The singlet O_h structure ($^1A_{1g}$) is found to be the global minimum either for the anion Li_6B^- or for the cation Li_6B^+, in agreement with earlier studies. For the neutral radical Li_7B, our calculated results are also consistent with previous reports [18,20] that the pentagonal bipyramid structure (D_{5h}, $^1A_1'$) is the global equilibrium structure. The C_{3v} structure of Li_7B ($^1A_1$) is found to be the second lowest-energy isomer with a relative energy of 4.3 kcal/mol (at the CCSD(T)/aug-cc-pVTZ level). Geometrical parameters and vibrational frequencies for the lowest-lying isomers summarized in Table 1 point out that there are small differences in geometries when using various methods. The B–Li distances in different clusters vary from 2.179 to 2.313 Å, that are close to that of the diatomic BLi (2.174 Å) [20]. The calculated stretching frequencies of the Li_5B (C_{4v}, $^1A_1$), Li_6B^+ (O_h, $^1A_{1g}$), Li_6B^- (O_h, $^1A_{1g}$), and Li_7B (D_{5h}, $^1A_1'$) are equal to 575, 546, 575 and 591 cm^{-1}, respectively, that are quite large as compared to those of the series of Li_nB clusters reported [20].

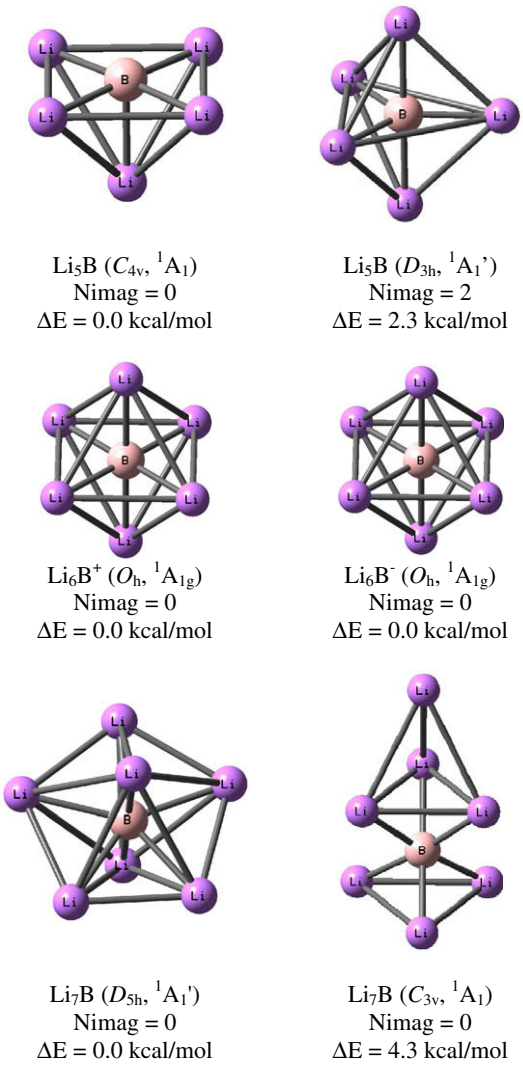

Fig. 1. Shape of the optimized structures for the clusters Li_5B, Li_6B^+, Li_6B^- and Li_7B. Relative energies (ΔE, kcal/mol) are obtained from CCSD(T)/aug-cc-pVTZ+ZPE calculations.

Some energetic properties of clusters were studied to measure their stability. The HOMO–LUMO gaps of the global minimum Li_5B and Li_7B amounts to 1.44 and 1.69 eV, respectively. The vertical ionization energy (vIE) of Li_5B, which is calculated as the energy difference between the neutral (C_{4v}, $^1A_1$) and the cation (C_{4v}, $^2A_1$) at the neutral geometry is 4.57 eV, whereas the vIE of Li_7B is 4.28 eV. As compared to the corresponding values ~4 eV of their neighbors in the series of Li_nB clusters [20], these energetic properties correlate with the fact that the neutrals Li_5B and Li_7B are more stable systems.

To probe the relative stability of the clusters considered, the energetic properties of clusters Li_nB (n = 1–8) were examined in

Table 1
Geometrical parameters and harmonic vibrational frequencies of global minima at B3LYP, MP2 and CCSD(T) methods with the aug-cc-pVTZ basis set.

Structures	r(Li–B) (Å)	r(Li′–B) (Å)	Frequencies(B3LYP) cm^{-1}
Li_5B (C_{4v}, $^1A_1$)	B3LYP = 2.093 MP2 = 2.129 CCSD(T) = 2.179	B3LYP = 2.246 MP2 = 2.150 CCSD(T) = 2.274	575, 575, 438, 433, 432, 264, 253, 253, 196, 196, 174, 118
Li_6B^+ (O_h, $^1A_{1g}$)	B3LYP = 2.124 MP2 = 2.178 CCSD(T) = 2.197		546, 546, 546, 420, 415, 415, 267, 267, 267, 226, 226, 226, 178, 178, 178
Li_6B^- (O_h, $^1A_{1g}$)	B3LYP = 2.119 MP2 = 2.182 CCSD(T) = 2.190		575, 575, 575, 412, 403, 403, 201, 201, 201, 200, 200, 200, 157, 157, 157
Li_7B (D_{5h}, $^1A_1'$)	B3LYP = 2.231 MP2 = 2.296 CCSD(T) = 2.313	B3LYP = 2.124 MP2 = 2.181 CCSD(T) = 2.195	591, 502, 502, 406, 367, 347, 347, 270, 270, 264, 264, 219, 180, 180, 170, 170, 81, 81

term of the average binding energy (E_b), second-order difference (Δ^2E) and dissociation enthalpies that are defined as follows:

$$E_b = [nE(\mathrm{Li}) + E(B) - E(\mathrm{Li}_nB)]/(n+1), \quad (1)$$

$$\Delta^2E(\mathrm{Li}_nB) = E(\mathrm{Li}_{n-1}B) + E(\mathrm{Li}_{n+1}B) - 2E(\mathrm{Li}_nB). \quad (2)$$

The plots of E_b, Δ^2E and dissociation enthalpies for two dissociated channels ($Li_nB \rightarrow Li_{n-1}B + Li$, $Li_nB \rightarrow Li_n + B$) are depicted in Fig. 3, whereas the calculated energetic values are summarized in supporting information. It can easily be observed that the average binding energies increase with an increasing number of lithium atoms, and the highest value is attained for Li_6B. The plot of second-order difference reveals two remarkable peaks at Li_5B and Li_7B that indicate a high stability of these clusters as compared to their neighbors. Additionally, it is fascinating to note that the dissociation enthalpy of $Li_5B \rightarrow Li_4B + Li$ is highest as compared to corresponding values of other remains in the dissociation channel $Li_nB \rightarrow Li_{n-1}B + Li$. For second dissociation channel $Li_nB \rightarrow Li_n + B$, the highest value of dissociation enthalpy is found at the Li_7B. These predictions provide a further support for our discussion about the high stability of the neutrals Li_5B and Li_7B.

The high symmetry cation Li_6B^+ (O_h, $^1A_{1g}$) was reported to be highly stable species within the series of cationic clusters Li_nB^+ [21]. According to our calculations, the HOMO–LUMO gap of Li_6B^+ is equal to 2.43 eV (earlier value being 2.36 eV), while the vertical attachment energy (vAE) of the cation Li_6B^+ that is the difference between the total energies of the cation Li_6B^+ (O_h, $^1A_{1g}$) and the neutral Li_6B (O_h, $^2A_{1g}$) at the cation optimized geometry, is 3.82 eV (previous value being 3.75 eV [21]). The anion Li_6B^- has not been reported in previous studies. Its HOMO–LUMO gap of 1.67 eV is similar to the values of 1.44 eV for Li_5B and 1.69 eV for Li_7B. Additionally, the global minimum of Li_6B^- is of high symmetry (O_h, $^1A_{1g}$), and exhibits an electronic structure similar to that of the highly stable species Na_6Pb [9].

3.2. Evaluation of the aromatic character

Aromaticity is an important measure to evaluate stability of compounds. In spite of the fact that the concept of aromaticity is still not well defined, it is widely applied in the chemical literature [33]. We perform an evaluation of aromaticity of clusters by analysing the canonical molecular orbital (CMO) and the nucleus independent chemical shifts indices (NICS) indices. The NICS is based on magnetic shieldings [34], and a negative NICS value suggests an aromaticity, whereas the positive NICS values reveal an antiaromaticity and a nonaromaticity is characterized by NICS values close to zero. Because the NICS values are largely influenced by

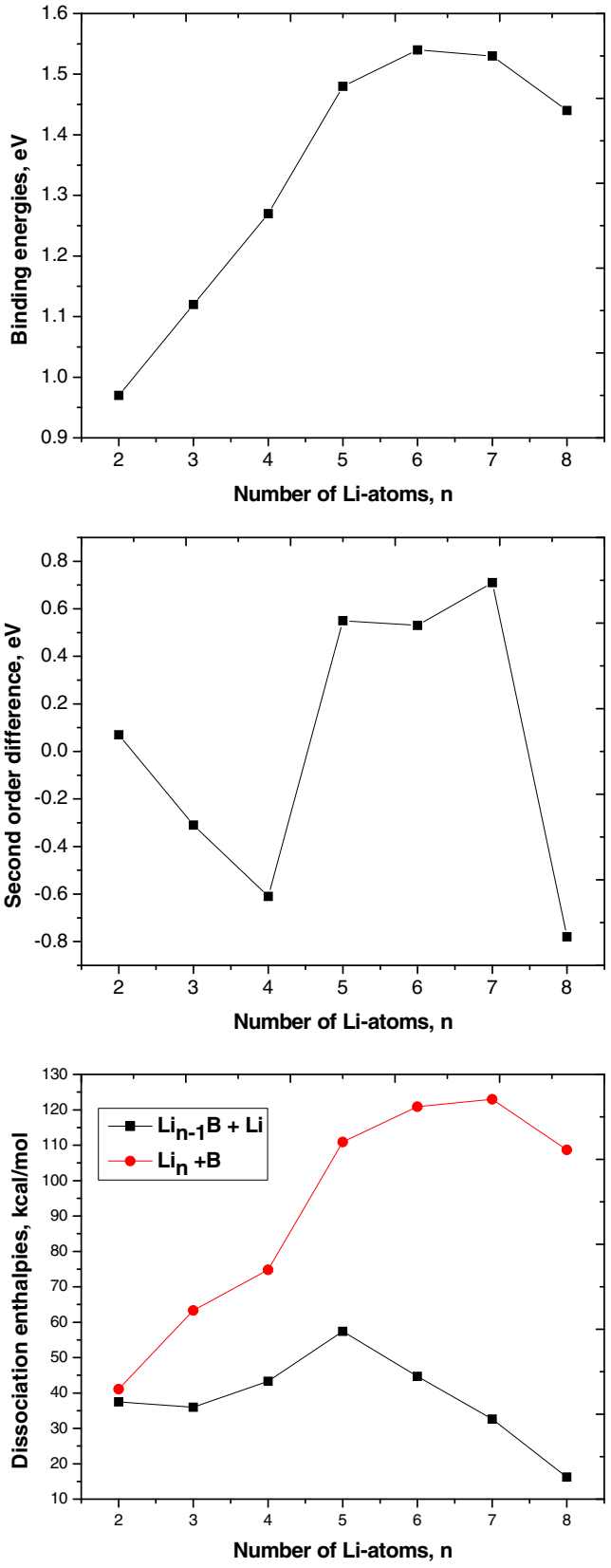

Fig. 2. The plots of average energy, second-order difference and dissociation enthalpies of clusters Li_nB (n = 2–8).

electrons in bonds, lone pairs and the core electrons [33], we consider the NICS(0), NICS(1) and NICS(2) values where the reference ghost atoms are placed at positions of 0, 1 and 2 Å above either the

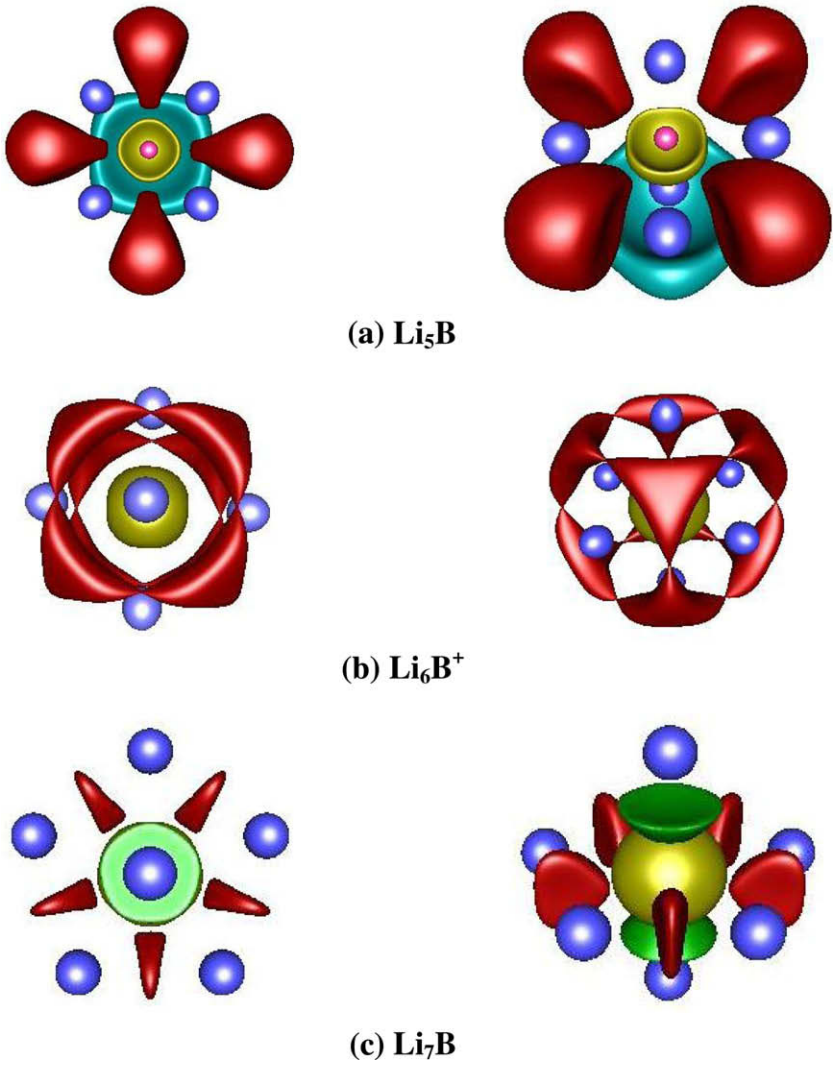

Fig. 3. pELI-D contributions of the valence orbitals in (a) Li_5B (C_{4v}, $^1A_1$), (b) Li_6B^+ (O_h, $^1A_{1g}$), and (c) Li_7B (D_{5h}, $^1A_1'$).

four-membered ring plane (for Li_5B and $Li_6B^{+/-}$), or the five-membered ring plan (for Li_7B).

The MO analysis of the ground state Li_5B (C_{4v}, $^1A_1$) shows that its HOMO is a globally delocalized π-orbital, and the three σ-orbitals (HOMO−1 (degenerate) and HOMO−2) are responsible for bonding. Consequently, the neutral Li_5B (C_{4v}, $^1A_1$) can be regarded as an σ-aromatic system that satisfies the Hückel rule of $4n + 2$ electrons. NICS calculations at the B3LYP/6-311+G(d) level reveal the highly negative values (NICS(0) = −15.7, NICS(1) = −15.8, and NICS(2) = −58.2) that are consistent with high aromatic character of the species.

The NICS value of the cation Li_6B^+ is also highly negative (NICS(1.0) = −21.1, NICS(2.0) = −47.0) that suggests a strongly aromatic structure. It is remarkable that although it possesses eight valence electrons (like its isoelectronic Li_5B), the cation Li_6B^+ has six globally delocalized π-electrons distributed over three degenerated π-orbitals, and that makes it a π-aromatic species. Following attachment of two excess electrons to the LUMO of Li_6B^+, the resulting anion Li_6B^- possesses two globally delocalized σ-electrons and six globally delocalized π-electrons. Consequently, the anion Li_6B^- is considered as a doubly σ and π-aromatic species in which each electron system satisfies the $4n + 2$ electrons rule. The NICS values for the anion Li_6B^- are highly negative (NICS(1.0) = −27.5 and NICS(2.0) = −54.6) that support this prediction.

For the neutral Li_7B (D_{5h}, $^1A_1'$), our calculations point out that the structure is also aromatic with very highly negative NICS values (NICS(1.0) = −25.9; NICS(2.0) = −49.5). The three orbitals (HOMO−2 (degenerate) and HOMO−3) are responsible for bond formation in the five-membered ring. While the HOMO−1 is a global σ-orbital, the HOMO is a global π-orbital. These two orbitals make the neutral (D_{5h}, $^1A_1'$) doubly (σ and π) aromatic as they contain two delocalized σ electrons and two delocalized π-electrons.

3.3. Electron localizability indicator (ELI)

Another way of probing the chemical bonding and electron delocalization is to consider the electron localizability indicator (ELI). The ELI plots for structures Li_5B and Li_7B are depicted in Fig. 3. The localization domains of lithium (given in cyan) and boron (in light red) are mainly composed of core orbitals. The isosurfaces of p-ELI distribution for the neutral Li_5B reveal that the red-colored localization domains arise from p_x and p_y-orbitals, whereas the green-colored domain is composed of p_z-orbital. Consequently, it was expected that the latter is responsible for its aromaticity. The NICS value of the neutral Li_5B is increased from NICS(0) = −15.7 to NICS(2) = −56.2, that is consistent with the above prediction. A similar analysis for Li_7B can be obtained that the p_x- and p_y-orbitals are responsible for bond formation, whereas

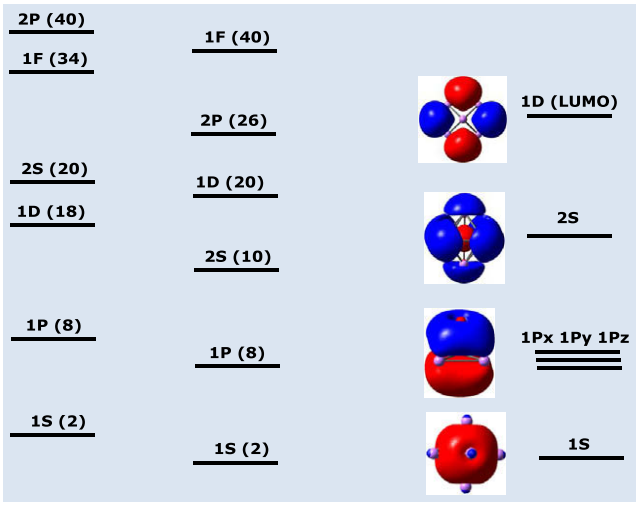

Fig. 4. The energetic ordering of valence orbitals of the two-step PSM and isosurfaces (isovalues of 0.02 a.u.) of the MOs of the Li_6B^- (O_h, $^1A_{1g}$).

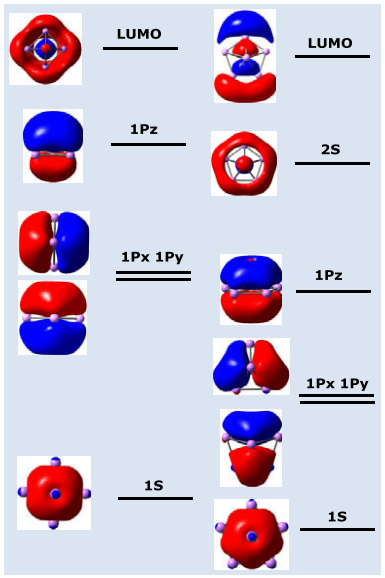

Fig. 5. Isosurfaces (isovalues of 0.02 a.u.) of the MOs of the Li_5B (C_{4v}, $^1A_1$) and Li_7B (D_{5h}, $^1A_1'$). The LUMO of Li_5B corresponds to the 2S shell, and the LUMO of Li_7B to the 1D shell.

the added s-orbitals (their domains is not presented here) distributed as a lone pair of lithium atoms are responsible for its aromaticity.

The p-ELI plots of the cation Li_6B^+ (Fig. 2b) point out that the red domains composed of three degenerate p-orbitals are distributed globally over the whole skeleton that renders the system highly aromatic. Additionally, it is obvious that there is presence of eight localized basins distributed on eight faces of the octahedral cation Li_6B^+ that form three-center bonds, and give a support for the high stability of this structure. There is negligible difference between the p-ELI plots of Li_6B in both cationic and anionic states. Similar to the case of Li_7B, added s-orbital (HOMO) of the anion Li_6B^- was delocalized as a lone pair of lithium atoms and contribute to the enhanced aromaticity of the anion Li_6B^-.

3.4. Phenomenological shell model (PSM)

We now rationalize the electronic structure of the clusters Li_5B, Li_6B^+, Li_6B^- and Li_7B within the framework of the PSM. The energetic ordering of the valence molecular orbitals of the Li_6B^- anion in conjunction with the ordering of the model is shown in Fig. 4. Similar correlations for the clusters Li_5B and Li_7B are depicted in Fig. 5. The three higher-lying orbitals (HOMO and degenerate HOMO−1) show a p-character, whereas the HOMO−2 is an s-orbital. The LUMO of Li_5B turns out to be an s orbital, and contributes predominantly to the 2S shell orbital. As a consequence, the neutral Li_5B is consistent with the configuration ($1S^2$ $1P^6$) of the PSM. A similar observation was found for the cation Li_6B^+ in which the three degenerate p-orbitals and one s-orbital (HOMO−1) are fully occupied by eight valence electrons, whereas its LUMO is an s-orbital, and contributes to the 2S shell orbital. This distribution is again consistent with the PSM configuration of ($1S^2$ $1P^6$).

For systems of 10 valence electrons including Li_6B^- and Li_7B, addition of one B atom that is a more electronegative element as compared to lithium results in a perturbation of the energy ordering of the valence orbitals taking part in the PSM. Thus, the systems possessing 10 valence electrons can be accounted for with the PSM configuration of ($1S^2$ $1P^6$ $2S^2$). Fig. 5 shows that the neutral Li_7B has 10 valence electrons and they are in line with the PSM arrangement. Its HOMO and HOMO−3 are two s-orbitals, whereas its HOMO−1 can be regarded as a p_z-orbital and the degenerate orbital HOMO−2 is p_x and p_y-orbitals. A similar picture is also observed for the anion Li_6B^- in which the two excess electrons occupy the s-orbitals leading to the PSM configuration of ($1S^2$ $1P^6$ $2S^2$).

4. Conclusion

In this present theoretical study, we determined the geometries of the boron-doped clusters Li_5B, Li_6B^+ and Li_6B^- and Li_7B using the B3LYP and MP2 methods. The global minima for clusters were found and further confirmed by coupled-cluster theory CCSD(T) calculations. These clusters have large vertical ionization energies, large HOMO–LUMO gaps and high degree of aromaticity as compared to the other members of the series of clusters Li_nB. In particular, we have demonstrated that the electronic structure of these species, and thereby their high stability, can perfectly be accounted for by the phenomenological shell model.

Acknowledgments

We are indebted to the KULeuven Research Council (GOA, IDO and IUAP programs). T.B.T. thanks the Arenberg Doctoral School of for a scholarship. M.T.N. thanks the HoChiMinh Institute for Computational Science and Technology (ICST, Viet Nam) for support.

Appendix A. Supplementary material

Supplementary data associated with this article can be found, in the online version, at doi:10.1016/j.cplett.2010.02.036.

References

[1] R. Ferrando, J. Jellinek, R.L. Johnston, Chem. Rev. 108 (2008) 845.
[2] Z. Chen, J. Am. Chem. Soc. 128 (2006) 12829.
[3] C. Brechingac, P. Cahuzac, J.P. Poux, Chem. Phys. Lett. 127 (1986) 445.
[4] W.D. Knight, K. Clemenger, W.A. de Heer, W.A. Saunders, M.Y. Chou, M.L. Cohen, Phys. Rev. Lett. 52 (1984) 2141.
[5] W.D. Kight, W.A. de Heer, K. Clemenger, W.A. Sauders, Solid State Commun. 53 (1985) 445.
[6] W. Bouwen et al., Chem. Phys. Lett. 314 (1999) 227.
[7] K. Hoshino, K. Watanabe, Y. Konishi, T. Taguwa, A. Nakajima, K. Kaya, Chem. Phys. Lett. 231 (1994) 499.

[8] M.M. Kappes, P. Radi, M. Schar, E. Schumacher, Chem. Phys. Lett. 119 (1985) 11.
[9] C. Yeretzian, U. Rothlisberger, E. Schumacher, Chem. Phys. Lett. 237 (1995) 334.
[10] E. Janssens, S. Neukermans, P. Lievens, Curr. Opin. Solid State Mater. Sci. 15 (2004) 8.
[11] C. Yeretzian, J. Phys. Chem. 99 (1995) 123.
[12] C. Yeretzian, U. Rothlisberger, E. Schumacher, Chem. Phys. Lett. 237 (1995) 334.
[13] P. Dugourd et al., Phys. Rev. Lett. 67 (1991) 2638.
[14] E. Benichou, A.R. Allouche, M. Aubert-Frecon, R. Antoine, M. Broyer, Ph. Dugourd, D. Rayane, Chem. Phys. Lett. 290 (1998) 171.
[15] Z.Y. Jiang, K.H. Lee, S.T. Li, S.Y. Chu, Int. J. Mass Spectrosc. 253 (2006) 104.
[16] M.D. Deshpande, D.G. Kanhere, Phys. Rev. A 65 (2002) 033202.
[17] T. Baruah, D.G. Kanhere, Phys. Rev. A 63 (2001) 063202.
[18] K.A. Nguyen, K. Lammertsma, J. Phys. Chem. A 102 (1998) 1608.
[19] K.A. Nguyen, G.N. Srinivas, T.P. Hamilton, K. Lammertsma, J. Phys. Chem. A 103 (1999) 710.
[20] Y. Li, D. Wu, Z.R. Li, C.C. Sun, J. Comput. Chem. 28 (2007) 1677.
[21] Y. Li, Y.J. Liu, D. Wu, Z.R. Li, Phys. Chem. Chem. Phys. 11 (2009) 5703.
[22] W. Ekardt, Phys. Rev. B 29 (1984) 1558.
[23] M.J. Frisch et al., Gaussian 03, Revision C.01, Gaussian, Inc., Wallingford, CT, 2004.
[24] H.J. Werner et al., Molpro, version 2008.1, a package of *ab initio* programs.
[25] C. Lee, W. Yang, R.G. Parr, Phys. Rev. B 37 (1988) 785.
[26] J.A. Pople, J.S. Binkley, R. Seeger, Int. J. Quant. Chem. Symp. 10 (1976) 1.
[27] L.A. Curtiss, K. Raghavachari, P.C. Redfern, V. Rassolov, J.A. Pople, J. Chem. Phys. 109 (1998) 7764.
[28] A. Becke, K. Edgecombe, J. Chem. Phys. 92 (1990) 5397.
[29] F.R. Wagner, V. Bezuly, M. Kohout, Y. Grin, Chem. Eur. J. 13 (2007) 5724.
[30] T. Holtzl, E. Janssens, N. Veldeman, T. Veszpremi, P. Lievens, M.T. Nguyen, ChemPhysChem 9 (2008) 833.
[31] M. Kohout, Dgrid-4.2, Max-Planck Institut fur Chemische Physik und Fester Stoffe, Dresden, 2007.
[32] L. Laaksonen, J. Mol. Graph. 10 (1992) 33.
[33] I.A. Boldyrev, L.S. Wang, Chem. Rev. 105 (2005) 3716.
[34] P.V.R. Schleyer, H. Jiao, N.J.R.V.E. Hommes, V.G. Malkin, O.L. Malkina, J. Am. Chem. Soc. 119 (1997) 12669.